

1
2
3
4
5
6
7
8
9
10
11
12
13
14
15
16
17
18
19
20
21
22
23
24
25
26
27
28
29
30
31
32
33
34

**Drying of Carrots in a Fluidized Bed. II.
Design of a Model Based on a Modular Neural
Network Approach**

F. Cubillos* and A. Reyes

Chemical Engineering Department,
Universidad de Santiago de Chile, Santiago, Chile

21
22

ABSTRACT

23 The present paper deals with the design of a neural network type
24 model for drying of carrots, which includes the associated transport
25 mechanisms of the process. The model uses the operational variables
26 and the time as input parameters. Two sub-layers of linear and sig-
27 moidal nodes make up the hidden layer, to represent the external and
28 internal resistances to the diffusion of water vapors during the drying
29 process. The single output node weights the contribution of each
30 mechanism of the drying process to predict the exit moisture content
31 of the product. This model was used to predict the drying of carrot
32 particles in a mechanically fluidized bed dryer reported in a previous

35
36
37
38

*Correspondence: F. Cubillos, Chemical Engineering Department, Universidad
de Santiago de Chile, P.O. Box 10233, Santiago, Chile; E-mail: fcubillo@lauca.
usach.cl.

39
40

1185

41 DOI: 10.1081/DRT-120023175

0737-3937 (Print); 1532-2300 (Online)

42 Copyright © 2003 by Marcel Dekker, Inc.

www.dekker.com

43 paper [Reyes, A.; Alvarez, P.; Marquardt, F. Drying of carrots in a
44 fluidized bed: I.- effects of drying conditions and modeling. *Drying*
45 *Technology* **2002**, *20* (7), 1463–1483.]. Simulated drying curves
46 obtained with this model fits adequately the curves determined
47 experimentally for the most operation conditions, which would
48 indicate that this model is appropriate to be used for rough estima-
49 tions in the design, the selection of optimal operational conditions,
50 and the scaling up of dryers.

51 *Key Words:* Drying modeling; Neural networks; Drying
52 simulations.
53

54 INTRODUCTION

55
56
57
58 The drying of particulate solids is a complex operation, since it
59 involves the consideration of simultaneous heat and mass transfer,
60 together with the characteristics of the dryer, the nature of the feed
61 material, the type of the air/feed contact, and the way in which the
62 energy is added to the system. To model such a process, it is necessary
63 to have good estimates of the rate of drying, the coefficients
64 of heat transfer, and the time of residence in the dryer.^[2] This information
65 has to be complemented by a complete knowledge of the physical
66 characteristics as well as the physical-chemical properties of the solids
67 involved.

68 Correlations to estimate the involved parameters only cover the
69 traditional types of dryers. In general, they do not include data about
70 the secondary geometry of the equipment, the type, form, size and initial
71 moisture of the feed material, etc. The incorporation of these variables in
72 the process models has usually been in empirical forms.

73 Drying processes are usually divided into two periods:
74

- 75 1. Constant rate drying: In this first period, the drying rate is only
76 determined by external conditions (temperature, flow, and
77 humidity of the drying air).
- 78 2. Falling rate drying: In this period, the drying rate diminishes
79 continually and is determined by the internal flow, of liquid
80 and/or vapor, in response to the external conditions.

81
82 In both periods, drying takes place through different combinations of
83 different steps of diffusion of the moisture. In the case of foods, the usual
84 approach to modeling mass transfer is to use the concept of effective

85 diffusivity (D_e), which allows describing the diffusion of moisture by
86 Fick's second law:

$$87 \quad \frac{\partial X}{\partial \theta} = \nabla \cdot (D_e \nabla X) \quad (1)$$

89
90 Equation (1) can be integrated for different geometric forms and different
91 initial conditions for the boundary.^[3]

92 These solutions do have a phenomenological base, but they do not
93 include all the above-cited operational variables. An alternative to
94 this approach is the use of nonparametric models, which by the use of
95 arbitrary mathematical functions make it possible to describe the drying
96 process with the direct inclusion of the operational parameters of the
97 dryer.

98 Among these nonparametric models, the neural networks have
99 become interesting in the last few years due to their capacity to correlate
100 efficiently multidimensional non-linear spaces. Neural networks were
101 already applied to model drying processes by Huang and Mujumdar,^[4]
102 Heyd et al.^[5] and Jay and Oliver.^[6] Although the work of these authors
103 has demonstrated that neural networks can be used to predict drying pro-
104 cesses, their adjustment requires a great amount of experimental data, and
105 even so, they do not give any additional information about the mecha-
106 nism involved in the process. Due to the limited amount of data and
107 noise in the data, the network outputs may not conform to the process
108 constrains. This inconsistency becomes more severe as the network makes
109 predictions beyond the limits of the training data (extrapolates).

110 Currently, researchers are investigating several designs and training
111 approaches to include prior knowledge into neural networks.^[7] These
112 approaches exploit the knowledge available prior to receiving process
113 data and attempt to reduce the dependence on noisy and sparse data.
114 In one of their works,^[8] propose the following structures, as informed in
115 Table 1.

116 In *Design Approaches*, prior knowledge dictates model structure.
117 This reduces the dimensionality of the parameter space. In *Training*
118 *Approaches*, prior knowledge dictates the form of the parameter estima-
119 tion problem. This reduces the feasible region of the parameter space.

120 For drying processes, this prior knowledge can be included as a semi-
121 parametric design approach in the form of balance equations^[9,10] or as
122 modular design approach where the network structure is designed follow-
123 ing some process mechanism (or process concept). As an elaboration of
124 this last methodology,^[11,12] developed a so called Generalized Drying
125 Model (GDM), in which the architecture of the network was designed
126 to weight the contribution of the internal and external resistances in the

T1

127
128
129
130
131
132
133
134
135
136
137
138
139
140
141
142
143
144
145
146
147
148
149
150
151
152
153
154
155
156
157
158
159
160
161
162
163
164
165
166
167
168

Table 1. Structures combining previous knowledge with neural networks.

| Structure | Design approaches | | Training approaches | | |
|---------------|--|-----------------------------|--|--------------------------|---|
| | Modular | Semiparametric | | Objective function | |
| | | Serial | Parallel | | Inequality constraints |
| Advantages | May improve interpretability. Easier to train. | Guaranteed output behavior. | Network compensates for discrepancies between data and inexact parametric model. May enforce different constraints over different sub-regions. | Consistent outputs. | Preferred functional behavior. Improved generalization. |
| Disadvantages | Output behavior not guaranteed. Unstructured sub-networks. | Unstructured network. | Output behavior not guaranteed. | More difficult to train. | Difficult to determine appropriate form. Must determine regularized constant. |

169 process, giving good results for the simulation of the drying of fish meal
170 in an indirect dryer, when compared with experimental data.

171 In the present paper, the GDM structure was applied to model and
172 simulate the batch drying of carrots in a fluidized bed under different
173 operating conditions (air velocity and temperature). The drying of the
174 carrot particles is accompanied by significant volume contractions,
175 caused by changes in their microstructure due to gradients of moisture,^[13]
176 which creates complications in a phenomenological model of the process
177 based on equations. As it was mentioned, the GDM model can be ade-
178 quate to describe the drying profile considering the global aspect of the
179 operation, such as, input variables and transport resistances.

180

181

182

183

GDM NEURAL NETWORK ARCHITECTURE

184

185

186

187

188

189

190

191

192

193

194

195

196

197

198

199

200

201

202

203

204

205

206

207

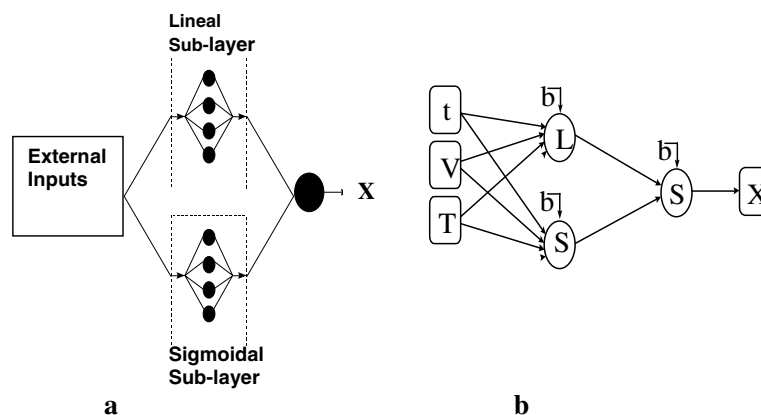
208

209

210

The architecture of the GDM network is based on the work of Cubillos et al.^[11] which defines a feed-forward neural network, in which the hidden layer is made up by two sub-layers, one of linear and the other of sigmoidal nodes, as shown in Fig. 1(a). In this architecture the inputs to the net are time and all the external variables of the drying process. The linear and sigmoidal sub-layers represent the external and internal resistances respectively, while the single output node weights both resistances to yield the solid's moisture content. So, the drying curve (moisture content vs. time) can be obtained for different operational conditions.

F1



209 **Figure 1.** Model architectures: (a) General GDM model; (b) Model selected in
210 this work.

1190

Cubillos and Reyes

211 In the GDM sigmoidal sub-layer, the activation functions in each
212 node are given by:

$$213 \quad S[f] = 1/(\exp(-f)) \quad (2)$$

214
215 Where “ f ”, the node confluence, expressed by:

$$216 \quad f = \Theta * U + b \quad (3)$$

217
218 U represents the input vector to the node, b the bias, and Θ , the synaptic
219 weights.

220 For the linear sub-layer, the activation functions are the node
221 confluence only, that is:

$$222 \quad L[f] = f \quad (4)$$

223
224 The GDM output, that is, the solid’s moisture content, is
225 obtained by:

$$226 \quad X = \Theta_2^L * L[f] + \Theta_2^S * S[f] \quad (5)$$

228

229

230

231

EQUIPMENT, MATERIALS, AND EXPERIMENTAL METHODS

232

233

234

Equipment

235

236

237

238

239

240

241

242

243

244

245

Materials

246

247

248

249

250

251

252

F2

The fluidized bed chamber (Fig. 2) consists of a truncated conical base section with a 0.25 m bottom diameter and a 0.5 m upper diameter (angle of 11°), and a 1 m high cylindrical column. The base section contained a blade agitator, connected through a vertical shaft to a 1/4 HP variable-speed motor. A motor of 10 HP powers the air blower. More details can be obtained in Reyes and Navarro.^[14]

The drying experiments were carried out with the Chantenay variety of carrots (*Daucus Carota*). Water washed carrots were peeled manually and cut into 3-mm slices by an electric sausage slicer, and then manually into 9 mm squares, which had a moisture content of 13.9 (kg water/kg d.b.). To minimize the enzymatic reactions, the samples were blanched in water for 8 min at 90°C, which resulted in an observed loss of 11% of the mass of the solids by dissolution, which agree with the observation by

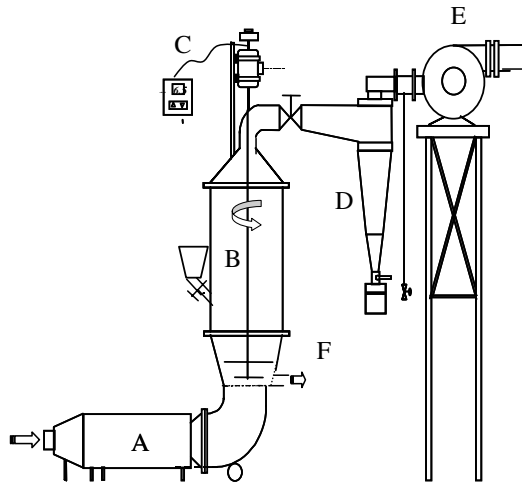


Figure 2. Flow sheet of the dryer. A. Heater, B. Fluidization chamber, C. Variable frequency motor, D. Cyclone, E. Centrifugal blower, F. Sampling port.

Kincal and Kayman,^[15] and which they assigned to sucrose diffusion and reduction of sugars, and which could be increased with the blanching time.

Drying Procedure and Determination of Particle Shrinking

A batch of 3 kg of the blanched parallelepiped particles, with a moisture content of $X_o \approx 15.4$ (kg water/kg d.b.), was dried at pre-established temperatures, air velocities and rate of agitation, with samples taken every 2 min at the beginning, and every 5 min in the later stages of the process. Lots of 10 or 20 particles of each sample were submerged in a toluene-containing burette, to determine their volume, and the moisture content was determined in similar additional lots by standard gravimetric methodology at 80°C.

RESULTS

In a previous paper,^[1] the experimental data was reported, corresponding to 26 drying runs. The mean experimental error reported was 6% where the mayor deviations were observed in the first 5 min of the drying, due to a certain heterogeneities of the bed, since at high moisture

295 content, the movement of the particles is not enough to guarantee a good
 296 fluidization. In this work, a set of 12 drying curves with different inlet
 297 temperatures (70, 90, 100, and 120°C), and air velocities (1.1, 1.7, and
 298 2.2 m/s) were selected, with 233 experimental data points. Mechanical
 299 agitation practically did not influence the drying curves, therefore this
 300 variable was not included in the present study.

301

302

303 GDM Model

304

305 The GDM architecture was synthesized considering time, air velocity,
 306 and inlet temperature as inputs, and the dimensionless moisture content
 307 (X) as output.

308 The two hidden sub-layers have linear and sigmoidal nodes with their
 309 corresponding biases.

310 The best architecture of the network was determined by looking
 311 for the optimal number of nodes in each hidden sub-layer, which mini-
 312 mizes the error between the predicted and the experimental moisture
 313 content. The design of the network, its programming and training were
 314 carried out by means of the neural network toolbox of Matlab.

315 The resulting architecture is shown in Fig. 1(b), where only a single
 316 node for each sub-layer in the network is adequate to reproduce the
 317 experimental process data. For this structure, the output of the network,
 318 expressed as moisture content, is given by the following equation:

$$319 \quad X = \Theta_2^L * L[\Theta_1^L * U + b^L] + \Theta_2^S * S[\Theta_1^S * U + b^S] \quad (6)$$

320

321 Output weights values are reported in Table 2. The values are 1.088 for
 322 the sigmoidal sub-layer and 2.627 for the linear sub-layer. These values
 323 indicate that both resistances are present in the process, and that the
 324 external resistance (convective) could be more important one.

T2

325

326

327 Prediction of the Drying Curve

328

329 In Fig. 3, the values determined experimentally for the exit moisture
 330 are compared with those calculated on the basis of the neural network

F3

331

332

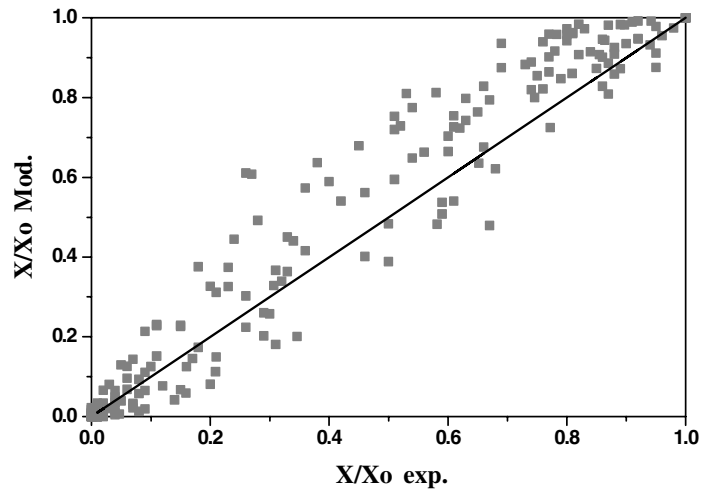
333 **Table 2.** Outputs weight values.

334

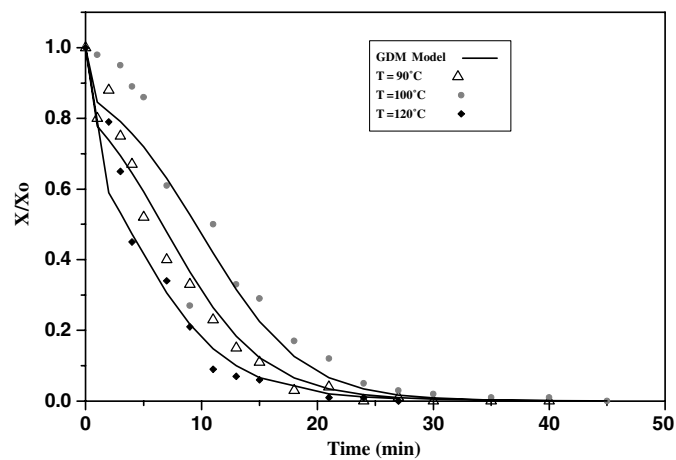
335

336

| Linear layer | Sigmoidal layer |
|----------------------|----------------------|
| $\Theta_2^L = 2.627$ | $\Theta_2^S = 1.088$ |



353 *Figure 3.* Experimental and simulated moisture content.
354



370 *Figure 4.* Experimental and modeled drying curves for $V=2.2$ (m/s).
371

372
373 with the selected architecture. It can be shown that the model is able to
374 fit reasonably the experimental data without biases and exhibits a good
375 performance in the extreme points. The total fit has a cumulative sum
376 squared error of 0.0052.

377 With the GDM model, it is possible to obtain the drying curves for
378 different operating conditions, as shown in Figs. 4 and 5, where the

F4 F5

379
380
381
382
383
384
385
386
387
388
389
390
391
392
393

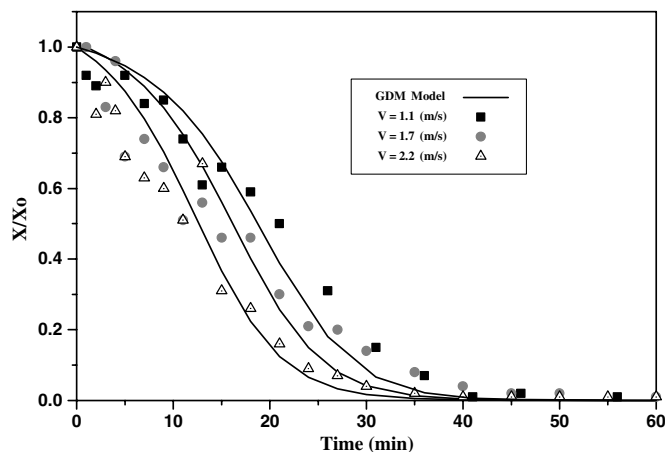


Figure 5. Experimental and modeled drying curves for $T = 70^{\circ}\text{C}$.

394
395
396
397
398
399
400
401
402
403
404
405
406
407
408
409
410
411

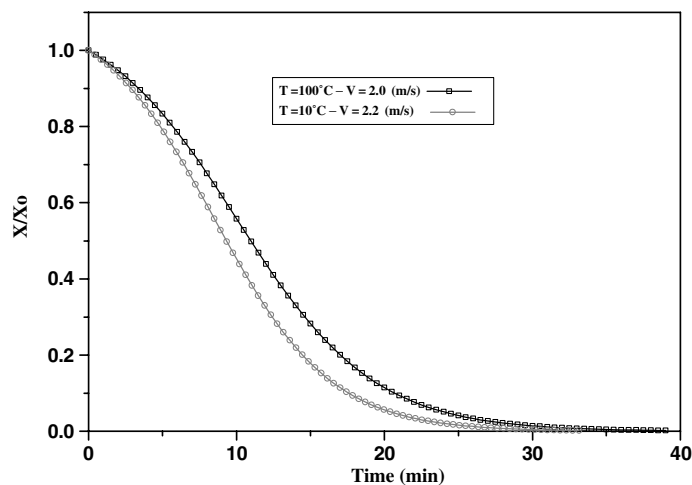


Figure 6. Simulated drying curves for others operation conditions.

412
413
414
415
416
417
418
419
420

experimental data are presented together with the calculated data for several air velocities and inlet air temperatures. Results show reasonable concordance between calculated and the experimental data, with maximum deviations for the prediction for 90°C , especially for the points collected before 5 min of drying. Besides, most of the predicted curves show the typical S-shape, which is characteristic of drying

421 processes with combined resistances, and Fig. 5 shows how they are
422 influenced by the air velocity.

423 In addition, Fig. 6 shows how the GDM model can be used to predict
424 drying curves for other operational conditions allowing the use for
425 optimal design and operations.

F6

426

427

428

CONCLUSIONS

429

430

431

432

433

434

435

436

437

438

439

NOMENCLATURE

440

441

442

443

444

445

446

447

448

449

450

451

452

453

454

455

456

457

458

459

ACKNOWLEDGMENTS

460

461

462

The authors wish to thank the financial support of projects FONDECYT # 1010700 and 1020041.

REFERENCES

- 463
464
465 1. Reyes, A.; Alvarez, P.; Marquardt, F. Drying of carrots in a fluidized bed: I.- effects of drying conditions and modeling. *Drying Technology* **2002**, *20* (7), 1463–1483.
466
467
468 2. Mujumdar, A. *Drying Technology in Agriculture and Food Sciences*; Science Publishers, Inc., 2000.
469
470 3. Crank, J. *The mathematics of diffusion*; Oxford Univ. Press: London, 1995.
471
472 4. Huang, B.; Mujumdar, A. Use of the neural networks to predict industrial dryer performance. *Drying Technology* **1993**, *11* (3), 525–541.
473
474
475 5. Heyd, B.; Rodriguez, G.; Vasseur, J. *Modeling of Drum Dryer using Neural Networks and Polynomial Models*, Drying 96-IDS'96: Poland, 1996; 323–330.
476
477
478 6. Jay, S.; Oliver, T. *Modeling and Control of Drying Processes Using Neural Networks*, Drying 96-IDS'96: Poland, 1996; 323–330.
479
480 7. Psychogios, D.; Ungar, L. A hybrid neural network-first principles approach to process modeling. *AIChE Journal* **1992**, *38*, 10.
481
482 8. Thompson, M.; Kramer, M. Modeling chemical processes using prior knowledge and neural networks. *AIChE Journal* **1994**, *40* (8).
483
484 9. Cubillos, F.A.; Álvarez, P.; Pinto, J.; Lima, E. Hybrid-neural modeling for particulate solid drying processes. *Powder Technology* **1996**, *87*, 153–160.
485
486
487 10. Zbicinski, Y.; Kaminski, W.; Ciesielski, K.; Strumillo, P. *Dynamic and Hybrid Model of Thermal Drying in a Fluidized Bed*, Proc. Drying 96-IDS'96, Poland, 1996.
488
489
490 11. Cubillos, F.; Mateo, J.; Vega, R. A generalized drying model with neural network structure. Proc. Inter-American Drying Conference SP. Brasil, 1997.
491
492
493 12. Mateo, J.; Cubillos, F.; Alvarez, P. Hybrid neural approaches for modeling drying processes for particulate solids. *Drying Technology* **1999**, *17* (4 and 5), 809–823.
494
495
496 13. Suzuki, K.; Kubota, K.; Hasegawa, T.; Osaka, H. Shrinkages in the dehydration of root vegetables. *J. Food Sci.* **1976**, *41*, 1189–1194.
497
498 14. Reyes, A.; Navarro, O. *Drying of Carrots in Fluidized Bed*, ENEMP 2001, Brazil, 2001 (in Spanish).
499
500 15. Kincal, N.S.; Kaymak, F. Modelling dry matter losses from carrots during blanching. *Journal of Food Process Engineering* **1987**, *9*, 201–211.
501
502
503
504